REDUCING DEPHOSPHORIZATION OF SiMnALLOY BY CaO-CaF_2 SLAG AND THE STABILITY OF Ca_3P_2 IN SLAG UNDER ATMOSPHERIC COOLING CONDITIONS

[1]Jae Hong Shin, [2]Joo Hyun Park

[1]School of Materials Science and Engineering, University of Ulsan, Ulsan, 680-749 Korea
[2]Department of Materials Engineering, Hanyang University
Ansan, 426-791 Korea, e-mail: basicity@hanyang.ac.kr

ABSTRACT

This study consists of experimental measurement of the phosphide capacity of the CaO-CaF_2 (-SiO_2) slag in equilibrium with SiMn alloy at 1823 K, and includes the thermodynamic analysis for the stability of reducing refining slags under various cooling conditions. Because Ca_3P_2, which is a reaction product of the reducing dephosphorization mechanism, is very active, the phosphine gas (PH_3), which is hazardous to environment as well as to human being, is evolved when it contacts to moisture. The phosphide capacity increased with increasing CaO concentration in the slag, followed by a constant value. The composition for the saturating capacity is in good accordance to the saturation content of CaO in the CaO-CaF_2 slag at 1823 K. When the slag disintegrated into fine powders not only due to the formation of dicalcium silicate but also due to the hydration of lime in the highly basic slags, the evolution of phosphine gas during cooling increased. When the Vee ratio (=CaO/SiO_2) of the dephosphorization slag is greater than about 1.35, lime and dicalcium silicate phases appeared during cooling cycle based on the CaO-SiO_2-CaF_2 phase diagram, resulting in an increase in the evolution rate of PH_3 gas due to an increase in the reaction area. However, when the Vee ratio of the slag is lower than about 1.35, the CaF_2, $Ca_4Si_2F_2O_7$ (cuspidine), and $CaSiO_3$ (wollastonite) phases appeared from the phase diagram, resulting in negligible amount of PH_3 evolution during cooling because the reaction between Ca_3P_2 and H_2O was restricted to the surface of bulk slag. Alternatively, the Ca_3P_2 phase was successfully transformed to the stable $3CaO{\cdot}P_2O_5$ phase by oxygen injection into the molten dephosphorization slag at high temperatures.

KEYWORDS: *Phosphide capacity, CaO–CaF_2 (–SiO_2) slag, SiMn alloy, Ca_3P_2 stability, Phosphine (PH_3) gas, Slag disintegration, Vee ratio, $3CaO{\cdot}P_2O_5$, Oxygen injection.*

1. INTRODUCTION

High manganese steels (10~25% Mn) are of interest due to their good mechanical properties including superior strength and good ductility [1]. Accordingly, the demand for ultra-low phosphorous manganese ferroalloys such as FeMn and SiMn alloys has recently increased. However, the conventional oxidizing dephosphorization technique is not applicable to Mn alloys because silicon or manganese will be oxidized before phosphorous under oxidizing conditions [2-4]. Therefore, the dephosphorization should be carried out under a strongly reducing atmosphere to produce a low phosphorus Mn alloys. The mechanism of reducing dephosphorization using lime-based highly basic fluxes has been reported by several authors [2-6].

However, because the calcium phosphide (Ca_3P_2), which is a reaction product of the reducing dephosphorization mechanism, is very active when it is exposured to moisture, the hazardous phosphine gas (PH_3) evolves [3, 5]. The equilibrium reaction of the emission of phosphine gas is as follows:

$$Ca_3P_2(s) + 3H_2O(g) = 3CaO(s) + 2PH_3(g) \quad (1)$$

$$Ca_3P_2(s) + 6H_2O(g) = 3Ca(OH)_2(s) + 2PH_3(g) \quad (2)$$

The Gibbs free energy changes of the formation of phosphine gas were calculated by using FactSage^{TM}6.2 software, which is a commercial thermochemical computing program [7, 8]. The emission of phosphine gas dominantly originates from the formation of CaO at temperature higher than about 803 K, whereas from the formation of $Ca(OH)_2$ at temperature lower than about 803 K. However, even in any cases, it is inevitable to evolve the PH_3 gas during cooling of slags containing Ca_3P_2 under moist atmosphere. Phosphine gas is hazardous to environment as well as to human being [9]. Inhalation is the most likely route of exposure to phosphine gas. Symptoms are non-specific and include irritation of the respiratory tract, headaches, dizziness, abdominal pain, sickness, and vomiting. Severe phosphine poisoning can cause convulsions, damage to the lungs, heart, liver and kidney, and death [9].

Therefore, this study consists of the distribution behavior of phosphorous between the CaO-CaF_2 (-SiO_2) slag and SiMn alloy melts at 1823 K, and includes the thermodynamic and kinetics analyses for the environmental stability of reducing refining slags under wet and dry cooling conditions based on the effect of slag composition on the evolution of PH_3 gas.

2. EXPERIMENTAL

A super-kanthal electric furnace was used for the equilibration of the CaO-CaF_2 (-SiO_2) slag and SiMn alloy melts. The temperature was controlled within ±2 K using a B-type thermocouple and a PID controller. The slag samples were prepared using reagent grade CaF_2 and CaO calcined from $CaCO_3$ at 1273 K for 10 hours. The initial composition of the slag in the CaO-CaF_2 system ranged from 5 to 25% CaO. The schematic diagram of the experimental apparatus is shown in previous articles [10].

The slag (7.0 g) and SiMn alloy (3.5 g) were held in graphite crucibles under a CO atmosphere to equilibrate. For reducing removal of phosphorous under a very low oxygen potential, CO gas was diluted with Ar, which was purified using silica gel also in addition to Mg turnings at 723 K. The oxygen partial pressure can be calculated based on the following reaction [11]:

$$C(s) + \frac{1}{2}O_2(g) = CO(g), \quad \Delta G^o = -114{,}450 - 85.8T \text{ (J/mol)} \quad (3)$$

With a CO/(CO+Ar) ratio of 0.25, the oxygen partial pressure is about 1.7×10^{-17} atm at 1823 K. After equilibrating for 12 hours, the slag samples were cooled under fully moisturized condition (direct contact with water spray), whereas the other samples were quickly quenched from 1823 K. Then, the samples were rapidly crushed for chemical analysis under inert atmosphere. The composition of metal samples was determined using ICP-AES and the equilibrium composition of slag was determined using XRF. The crystalline phases of solidified slags were identified using XRD analysis.

3. RESULTS AND DISCCUSION

3.1. Thermodynamics of Reducing Dephosphorization

In the present study, the distribution ratio of phosphorous between the slag and metal phases (L_P) was calculated from the following equation:

$$L_P = \frac{(\text{mass \% P})_{slag}}{[\text{mass \% P}]_{metal}} \quad (4)$$

In case of solidified samples under fully wet conditions, *i.e.* 100% relative humidity, the equilibrium content of phosphorous in slag phase $(\%P)_{slag}$ was calculated from eq. [5], assuming that the loss of phosphorous in slag phase fully originated from the formation of PH_3 gas by the reaction with moisture during solidification. The equilibrium content of phosphorous in dry-quenched slags was also estimated from eq. [5], because these samples also reacted with moisture, even though moisture was very small, *i.e.* lower than about 25% relative humidity.

$$(\text{mass \% P})_{slag} = \frac{[W_P^i - W_P^f]_{metal}}{W_S \cdot F_{liquid}} \times 100 \quad (5)$$

where, W_P is the weight of phosphorous and the superscripts 'i' and 'f', respectively, represent the initial and the final content of phosphorus in the metal, W_S is the weight of slag. F_{liquid} is the fraction of liquid phase of slag which was calculated by lever rule from CaO–CaF_2 binary phase diagram [12]. Consequently, when the CaO contents are 20 and 25%, F_{liquid} was estimated to be 0.99 and 0.93, respectively.

Figure 1 shows the effect of CaO content in the CaO–CaF_2 flux on the distribution ratio of phosphorous at 1823 K. Under the highly reducing conditions, phosphorous is expected to dissolve into the flux as phosphide ions as follows [2-6]:

$$[P] + \frac{3}{2}(O^{2-}) = (P^{3-}) + \frac{3}{4}O_2(g) \quad (7)$$

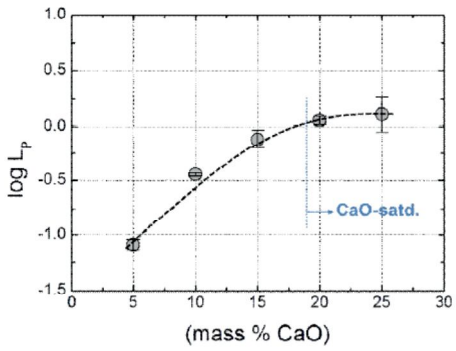

Figure 1: Effect of CaO content on the distribution ratio of phosphorous between the CaO-CaF_2 flux and SiMn melt at 1823 K

The phosphide capacity ($C_{P^{3-}}$) can be determined from equilibrium constant of Eq. (7) as follows.

$$C_{P^{3-}} = \frac{K_{[7]} \cdot a_{O^{2-}}^{1.5}}{f_{P^{3-}}} = \frac{p_{O_2}^{0.75}}{f_P} \cdot \frac{(\text{mass \% } P^{3-})}{[\text{mass \% P}]} \quad (8)$$

where $f_{P^{3-}}$ is the activity coefficient of the P^{3-} ions in the slag phase, f_P is the activity coefficient

of phosphorous in the SiMn alloy phase, p_{O_2} is the oxygen partial pressure, and $a_{O^{2-}}$ is the activity of O^{2-} ion, i.e. basicity of the slag. From eq. [9], the phosphorus distribution ratio is a function of phosphide capacity, stability of phosphorus in metal, and oxygen potential as follows:

$$L_P = \frac{f_P}{p_{O_2}^{0.75}} \cdot \frac{K_{[7]} \cdot a_{O^{2-}}^{1.5}}{f_{P^{3-}}} = \frac{f_P}{p_{O_2}^{0.75}} \cdot C_{P^{3-}} \tag{9}$$

Thus, the distribution ratio of phosphorous increases with increasing phosphide capacity of slag at a fixed oxygen potential. The L_P increases with increasing CaO content up to about 20%, which is mainly due to an increase in the basicity of the flux. However, it remains constant at CaO content greater than about 20%, where the flux is saturated by solid lime from the CaO-CaF_2 binary phase diagram,[12] indicating that the activity of free O^{2-} ions is approximately constant, assuming that $a_{O^{2-}}$ is proportional to a_{CaO} in the flux [2-4, 6, 10, 13-15].

3.2. Influence of CaO Content on the Emission of PH_3 Gas under Wet Conditions

Assuming that the loss of phosphorous in slag phase is fully originated from the formation of PH_3 gas by the reaction with moisture during solidification, the quantity of phosphine gas evolved (N_{PH_3}) can be calculated by Eq. [10]. That is, the emission of phosphine gas was calculated by the difference in the phosphorous content in slag before and after cooling. Because one mole of phosphine gas corresponds to one mole of phosphorous,

$$N_{PH_3} = \frac{W_S \cdot \{(\text{mass \% P})^{b/c} - (\text{mass \% P})^{a/c}\} \cdot 100}{M_P} \tag{10}$$

where the $(\text{mass\% P})^{b/c(=\text{before cooling})}$ was obtained from eq. [5] and $(\text{mass \% P})^{a/c(=\text{after cooling})}$ was from chemical analysis, and M_P (=30.97 g/mol) is the atomic weight of phosphorous. According to eq [1], the driving force of the forward reaction increases with increasing partial pressure of H_2O, whereas it decreases with increasing the activity of CaO in slag. Thus, the emission of phosphine gas is affected by these two factors.

Figure 2 shows the effect of CaO content on the amount of phosphine gas evolved which was normalized with reference to the dry-quenched samples.

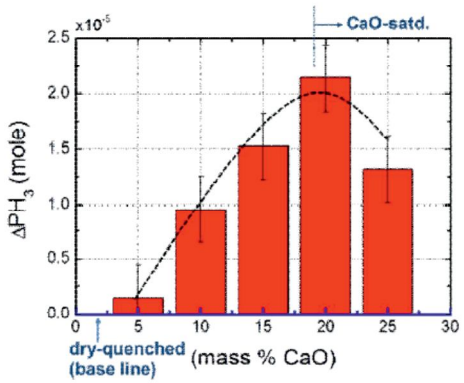

Figure 2: Effect of CaO content on the evolution of phosphine gas under wet conditions

In the lower CaO content region, viz. a_{CaO}<1.0, the phosphine gas was evolved due to the large potential of H_2O which is greater than that of CaO. However, even in the higher CaO content region, viz. a_{CaO}=1.0, the phosphine gas is still evolved, which is contradictory to the thermodynamic expectation. The reason for this discrepancy is discussed in the following sections.

3.3. Influence of Disintegration of Slag on the Emission of PH_3 Gas

When the CaO content is greater than about 15%, the slag was disintegrated into fine powders during cooling. The powdery slag in the CaO-CaF_2-SiO_2 slag is formed by two factors. Firstly, if CaO (lime) is crystallized during solidification under wet conditions, the hydration of CaO occurs, resulting in the volume expansion of slag [16]. Secondly, if Ca_2SiO_4 (dicalcium silicate) is crystallized during solidification, the Ca_2SiO_4 contributes to powdery slag because of the volume expansion by the phase transformation of Ca_2SiO_4 from β- to γ-phase at about 773 K [17].

Generally, the rate equation is functions of reaction surface area and driving force such as difference in concentration. Thus, the larger the surface area becomes, the faster the reaction will occur. That is, a disintegration of slag to fine powders results in a significant increase in surface area. The rate equation of the evolution of phosphine gas is as follows:

$$-\frac{dC_{Ca_3P_2}}{dt}=\frac{1}{2}\cdot\frac{d(C_{PH_3})}{dt}=\frac{A}{V}\cdot k_m\cdot(C^{i}_{Ca_3P_2}-C^{e}_{Ca_3P_2}) \tag{11}$$

where, k_m is rate constant, A and V are surface area and volume, respectively. $C_{Ca_3P_2}$ and C_{PH_3} are molar concentration of Ca_3P_2 and phosphine gas, respectively, the superscripts 'i' and 'e', respectively, represent the initial and the equilibrium molar concentration of Ca_3P_2. In the present study, the equilibrium molar concentration of Ca_3P_2 is assumed zero.

The surface area of powdery slag, which is constituted by large and small spherical particles, can be calculated by eq. [12] as follows [18]:

$$A=\frac{X_S\cdot(V\times f)}{V_S}\cdot A_S+\frac{X_L\cdot(V\times f)}{V_L}\cdot A_L \tag{12}$$

$$f=0.637+0.864\,X_S \tag{13}$$

where $X_{L\text{ or }S}$ is weight fraction of large or small particles, V is volume of bulk slag and $V_{L\text{ or }S}$ and $A_{L\text{ or }S}$ are unit volume and area of large or small particles, respectively. f is the fractional packing density. For two spherical powders with a large difference in particle size with an ideal fractional packing density of 0.637 [18].

Hence, the reaction rate of phosphine gas emission from powdery slag is determined by combining eqs. [11] to [13],

$$\frac{1}{Q}\cdot\frac{d(C_{PH_3})}{dt}=\frac{(r_S+(r_L-r_S)\cdot X_S)\cdot(0.637+0.864X_S)}{r_L\cdot r_S} \tag{14}$$

where Q is constant, and $r_{L\text{ or }S}$ is radius of large or small particles.

Figure 3 shows the effect of size ratio of large to small particles and the fraction of small particles on the evolution of phosphine gas. The more the slags become powdery, the larger the reaction surface area is expected, and thus the rate of gas evolution increases as a quadratic function. Therefore, if CaO or Ca_2SiO_4 are precipitated during solidification even in highly dry

atmosphere, the evolution of PH_3 gas could not be negligible.

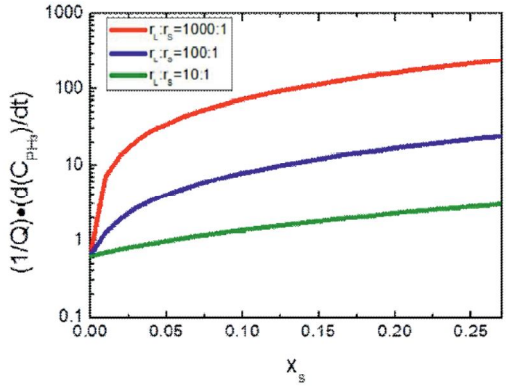

Figure 3: Effect of particle size ratio and fraction of small particle on the emission rate of PH_3 gas

The slag composition after dephosphorization is plotted on the CaO–CaF_2–SiO_2 ternary phase diagram as shown in figure 4 [19]. Solidification path can be predicted based on polythermal projection of the CaO-CaF_2-SiO_2 ternary phase diagram. Figure 4 also shows the schematic diagram of cooling path and the microstructure of solidified slag in each case 'a' and 'b' in phase diagram. For slags #1 and #2, the CaF_2 is primarily crystallized, followed by the nucleation and growth of SiO_2 (cristobalite). Finally the slag solidifies at the CaF_2-SiO_2-$CaSiO_3$ ternary eutectic composition. That is, the rate of phosphine gas emission is relatively low, because the solid compounds that contribute to the disintegration are not precipitated.

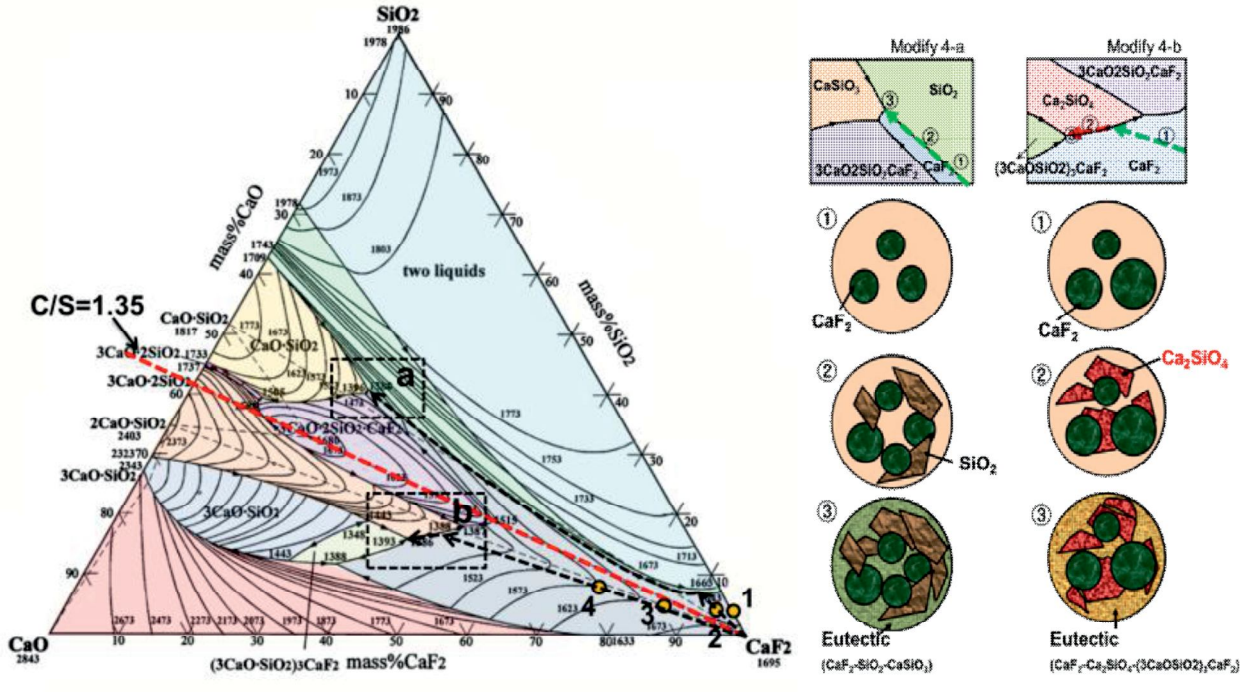

(a) (b)

Figure 4: (a) Slag composition after de-P reaction plotted on the CaO-CaF_2-SiO_2 phase diagram and (b) schematics of cooling path and the solidification structure of dephosphorization slags

On the other hand, for slags #3 and #4, the CaF_2 is primarily crystallized, followed by the

nucleation and growth of Ca_2SiO_4. After that, slag solidifies at the CaF_2-Ca_2SiO_4-$(3CaO{\cdot}SiO_2)_3CaF_2$ ternary eutectic composition. That is, the rate of phosphine gas emission is relatively high, because the solid compounds which contribute to the disintegration of slag, *e.g.* Ca_2SiO_4 are precipitated.

Consequently, when the Vee ratio (=CaO/SiO_2) of the dephosphorization slag is greater than about 1.35, the CaO (lime) and Ca_2SiO_4 (dicalcium silicate) phases precipitated during cooling cycle. This can be a reason for a decrease in between dry-quenched and wet-cooled 25% CaO samples in figure 2. That is, even it was directly quenched under dry atmosphere, the slag was disintegrated into fine powders, resulting in an emission of PH_3 gas before chemical analysis. Therefore, there was less difference in between dry-quenched and wet-cooled slag samples in highly basic compositions. However, when the Vee ratio of the slag is lower than about 1.35, the CaF_2, $CaSiO_3$ (wollastonite) and SiO_2 phases precipitated.

Figure 5 shows the result of XRD analysis of the dephosphorization slag of which initial composition is 5 and 25% CaO, respectively. The solid compounds at low CaO content slags were identified as mostly CaF_2 and $CaSiO_3$, whereas the compounds at high CaO content slags were confirmed as not only CaF_2 but also CaO, $Ca(OH)_2$ and Ca_2SiO_4. Thus, the present thermodynamics and kinetic discussions base on the phase equilibrium are in good agreement with the experimental result in this study.

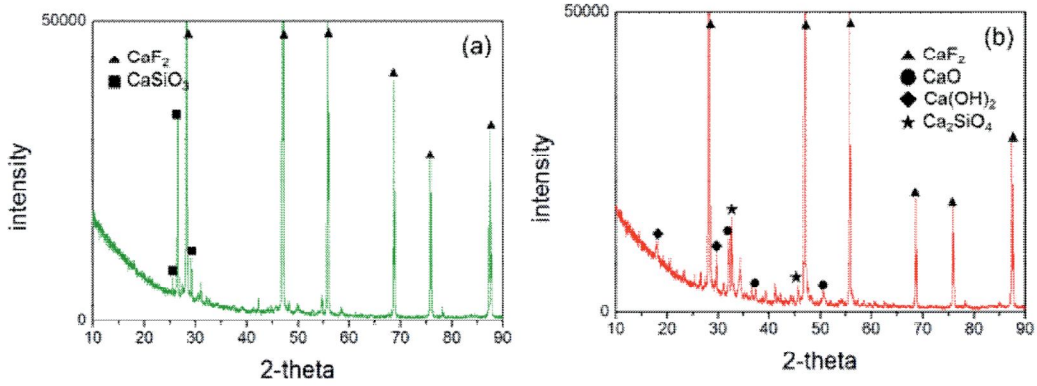

Figure 5: XRD analysis of the de-P slag of which initial composition is (a) 5 and (b) 25% CaO

Consequently, it is strongly recommended that reducing dephosphorization slags should be kept or treated under dry atmosphere. Furthermore, the Vee ratio of dephosphorization slag should be controlled to be lower than 1.35 during reducing refining reaction.

3.4. Conversion of Ca_3P_2 to $3CaO{\cdot}P_2O_5$ in Reducing Dephosphorization Slags by Oxygen Injection

Even though the above results are very useful to restrain the emission of phosphine gas from reducing dephosphorization slag during cooling, the problem due to phosphine emission at room temperature is still unsolved. Therefore, we tried to find a method to completely remove the Ca_3P_2 compound in reducing dephosphorization slag, which is the origin for the emission of PH_3 gas.

The Ca_3P_2 in molten reducing dephosphorization slag can be oxidized to the $3CaO{\cdot}P_2O_5$ phase at high temperature by oxygen injection as shown in eq. [15].

$$Ca_3P_2(s) + 4O_2(g) = 3CaO{\cdot}P_2O_5(s) \qquad (15)$$

The reducing dephosphorization slag (300 g), which was supplied from an industrial SiMn

refining process, was initially melted in the graphite crucible (OD: 56 mm, ID: 50 mm, HT: 96 mm) at 1773 K using a high frequency induction furnace with a graphite heater under a purified Ar-3%H_2 atmosphere. After the slag was melted, the power of the furnace was switched off, after which the slag was slowly cooled down. At this time, the gas was switched from Ar-H_2 gas mixture to O_2 gas, and then a stainless steel lance (OD: 6mm, ID: 4mm) for injecting O_2 gas (flow rate=1.0 l/min) was inserted into the molten slag and kept 5 mm above the bottom of the crucible. Strong agitation of the molten slag by O_2 gas injection resulted in fast attainment of the oxidation of reducing dephosphorization slag during cooling. After cooling, the crystalline phases of the solidified slags were identified using an XRD analysis.

Figure 6 show the results of XRD analyses for the as-received reducing dephosphorization slag and oxygen-treated slag, respectively. Both of the slags were mainly composed of calcium fluoride (CaF_2), wollastonite ($CaSiO_3$), cuspidine ($Ca_4Si_2F_2O_7$), dicalcium silicate (Ca_2SiO_4), iron oxide (Fe_2O_3) and manganese oxide (MnO) based on the reference peak from a JCPDS. The reducing dephosphorization slag was mainly CaO-CaF_2 system coupled with small amounts of SiO_2, Fe_2O_3, and MnO, those were formed during SiMn refining process. The cuspidine phase is believed to crystallize during solidification of the reducing dephosphorization slag.

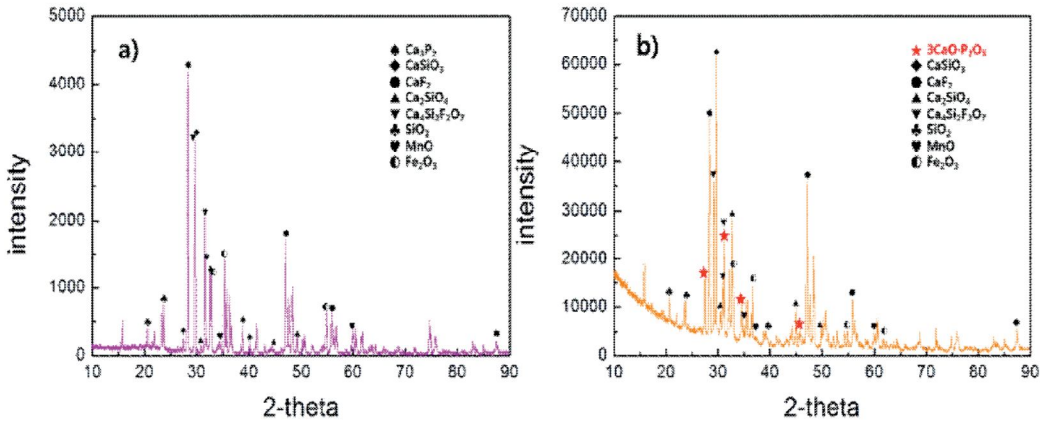

Figure 6: XRD pattern for the (a) as-received reducing dephosphorization slag from Mn smelting company and (b) the oxygen-treated reducing dephosphorization slag in the present experiments

It is very interesting in Figure 6 that the calcium phosphide (Ca_3P_2) was identified in the as-received reducing dephosphorization slag [20], whereas the tricalcium phosphate ($3CaO·P_2O_5$) compound was detected at the expense of Ca_3P_2 phase in the oxygen-treated slag. Consequently, from the present experiments, the Ca_3P_2 phase was successfully transformed to the $3CaO·P_2O_5$ phase by oxygen injection into the molten dephosphorization slag. This process can be potentially practiced in slag pot with the O_2-injection equipment in the ferroalloys smelter, resulting in the environmental friendly slag products instead of discarding or dumping the reducing dephosphorization slag at yard.

4. CONCLUSIONS

The distribution ratio of phosphorous between the CaO–CaF_2 (–SiO_2) slag and SiMn alloy melts at 1823 K was measured under strongly reducing atmosphere. Furthermore, thermodynamic and kinetics analyses were carried out for the environmental stability of reducing refining slags containing Ca_3P_2 under wet cooling conditions from the effect of slag composition on the evolution of PH_3 gas. The results of this study can be summarized as follows.

1. The distribution ratio of phosphorous between the $CaO–CaF_2$ ($–SiO_2$) flux and SiMn metal phases increased with increasing CaO concentration in the flux, followed by a constant value. The composition for the saturating distribution ratio of phosphorous is in good accordance to the saturation content of CaO in the $CaO–CaF_2$ flux at 1823 K. This means that the reducing refining mechanism was confirmed due to transfer of Ca from slag to metal phase by the reaction between CaO in the flux and Si in the alloy under strongly reducing conditions.

2. Despite of activity of CaO in the flux was unity at CaO > 20%, the emission of phosphine gas was still high, which is mainly due to the fact that the basic dephosphorization slag was disintegrated into fine powders. When the slag was disintegrated not only due to the phase transformation of dicalcium silicate but also due to the hydration of lime during cooling under wet conditions, the emission of phosphine gas significantly increased.

3. When the Vee ratio ($=CaO/SiO_2$) of the reducing dephosphorization slags is greater than about 1.35, the lime and dicalcium silicate phases precipitated during solidification, resulting in an increase in the emission rate of PH_3 gas due to an increase in the reaction area. However, when the Vee ratio of the slags is lower than about 1.35, the fluorite, cristobalite, and wollastonite phases appeared from the phase diagram, resulting in less amount of PH_3 emission during cooling because the reaction between Ca_3P_2 and H_2O was restricted to the surface of bulk slag.

4. The Ca_3P_2 phase was successfully transformed to the $3CaO{\cdot}P_2O_5$ phase by oxygen injection into the molten dephosphorization slag. This process can be potentially practiced in slag pot with the O_2-injection equipment in the ferroalloys smelter, resulting in the environmental friendly slag products instead of discarding or dumping the reducing dephosphorization slag at yard.

5. REFERENCES

[1] K.H. So, J.S. Kim, Y.S. Chun, K.T. Park, Y.K. Lee and C.S. Lee: ISIJ Int., 2009, vol. 49, pp. 1952-59.
[2] H. Momokawa and N. Sano: Metall. Trans. B, 1982, vol. 13B, pp. 643-44.
[3] S. Tabuchi and N. Sano: Metall. Trans. B, 1984, vol. 15B, pp. 351-56.
[4] S. Tabuchi and N. Sano: Tetsu-to-Hagane, 1985, vol. 71, pp. 687-92.
[5] H. Fujiwara, J.Y. Liang, K. Takeuchi and E. Ichise: Mater. Trans. JIM, 1996, vol. 37, pp. 923-26.
[6] J.H. Shin and J.H. Park: Metall. Mater. Trans. B, 2012, vol. 43B, pp.1243-46.
[7] www.factsage.com.
[8] C.W.Bale, E. Belisle, P. Chartrand, S.A. Decterov, G. Eriksson, K. Hack, I.H. Jung, Y.B. Kang, J. Melancon, A.D. Pelton, C. Robelin and S. Petersen: Calphad, 2009, vol. 33, pp. 295-311.
[9] J.L. Burgess: J. Toxicology – Clinical Toxicology, 2001, vol. 39, pp. 165-68.
[10] K.Y. Ko and J.H. Park: Metall. Mater. Trans. B, 2011, vol. 42B, pp. 1224-30.
[11] E.T. Turkdogan: Physical Chemistry of High Temperature Technology, Academic Press, New York, NY, 1980, pp. 1-24.
[12] W.G. Seo, D. Zhou and F. Tsukihashi: Mater. Trans., 2005, vol. 46, pp. 643-50.
[13] G.H. Park, Y.B. Kang and J.H. Park: ISIJ Int., 2011, vol. 51, pp. 1375-82.
[14] J.H. Park and G.H. Park: ISIJ Int., 2012, vol. 52, pp. 764-69.
[15] K.Y. Ko and J.H. Park: Metall. Mater. Trans. B, 2012, vol. 43B, pp. 440-42.
[16] D. Min, H. Dongwen, L. Xianghui, T. Mingshu: Cem. Concr. Res., 1995, vol. 25, pp. 440-48.
[17] C. Remy, D. Andrault: J. Am. Ceram. Soc, 1997. vol. 80, pp. 851-60.
[18] R.M. German: Powder Metallurgy Science, Metal Powder Industries Federation, New Jersey, 1994, pp. 166-71.
[19] T. Watanabe, H. Fukuyama, K. Nagata: : ISIJ Int., 2002, vol. 42, pp. 489-97.
[20] L.L. Pytlewski and E.R. Nixon: Inorg. Chem., 1963, vol. 2, pp. 763-64.